Lidar Investigation of Infiltration Water Heterogeneity in the Tamala Limestone, Southwest Western Australia

EP41B-3514

Kashif Mahmud[1], Gregoire Mariethoz[1,2], Pauline C. Treble[3], Andy Baker[1]

[1] Connected Waters Initiative Research Centre, UNSW Australia, Sydney, NSW, Australia
[2] Institute of Earth Surface Dynamics, University of Lausanne, Switzerland
[3] Institute for Environmental Research, Australian Nuclear Science and Technology Organisation, Lucas Heights, NSW, Australia

Contact: kashif.mahmud@unsw.edu.au
www.civeng.unsw.edu.au/current-students/research/kashif_mahmud

Background

Understanding matrix, fracture and conduit flow from 3-D information enhances our knowledge of the karst aquifer. Dense 3-D point clouds are increasingly used as highly detailed input datasets. Caves make it possible to enter the aquifer to directly capture 3-D point clouds to study a part of karst flow system. Analysis of caves using Lidar has been growing worldwide in recent years. However, so far Lidar data has not been used to perform quantitative morphological analysis of karstic features. There is a need to investigate the use of Lidar data, as well as the methods needed to process this kind of information. By performing a morphological analysis of karstic features based on Lidar data, we try to understand groundwater flow processes through saturated conduits, fractures and the matrix, and how they are expressed in the geological structures.

Site description

Our field site, Golgotha Cave (36.10°S 115.05°E, Fig 1A), is in aeolianites of Quaternary age: wind-blown calcareous sands that have deposited widely around the coast of SW Australia. The cave is 200m long and up to 25m wide, and the dune limestone is 20-30m thick over the monitoring sites in the cave (Fig 1B). The long cave chamber was originally formed by vadose zone waters and subsequent widened by ceiling collapse. Site 1 is located approx. 60m into the cave and sites 2 and 3 are located approx. 20m further into the cave within a second large chamber which appears to be less stable than site 1, as evidenced by roof-collapse, dense rubble on the floors and small breakdown chambers in the walls and ceilings.

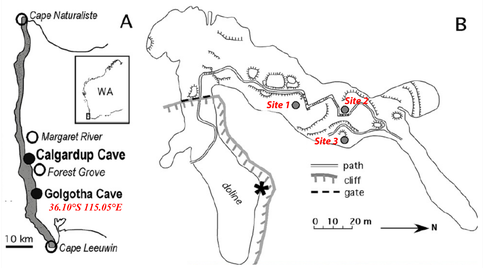

Fig 1: (A) Southwest Western Australia (SWWA) map showing coastal belt of dune calcarenite [Treble et al., 2013] (inset figure indicates SWWA region). (B) Plan view of Golgotha cave map showing all 3 Sites.

Objectives

1. Integrate Lidar data to build up a stalactite morphological model based on stalactite size and shape.
2. Relate stalactite density variations with the topographic elevation of the cave ceiling, potentially indicating the groundwater flow distribution governed by hydraulic gradient deviations.
3. Develop a relationship between stalactites length and diameter.

Approach and Methodology

1. For scanning the geological pattern we placed the lidar scanner at a few selected points at all sites.
2. The Lidar data has 1mm resolution, and we subsampled the resolution to a lower level of 1cm to reduce the number of data points, to minimize the data storage and computational effort.
3. From the cloud of scan points we further crop the relevant portion of cave ceiling comprising the stalactites for sites 1, 2 and 3. Fig 2 illustrates this in 3D with the stalactite distribution.

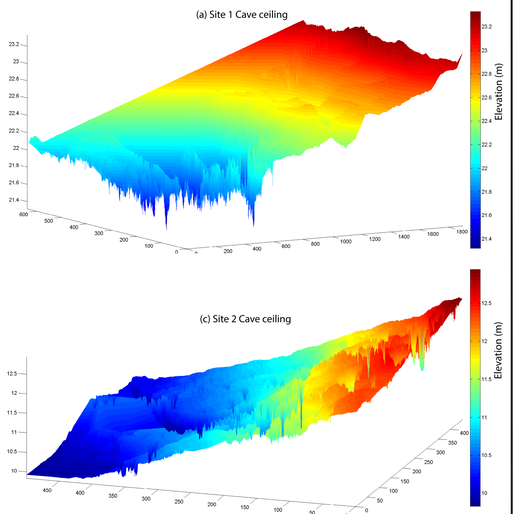

Fig 2: Different sites ceilings with stalactite distribution. Only showing data from site 1-2 to illustrate method. Ceiling sizes: site 1 = 19.0m by 6.4m, site 2 = 4.5m by 5.0m (Red specifies the higher ceiling elevation).

4. Stalactites were identified in the Lidar data by first subtracting a smoothed surface (created with a moving average of 40x40 cm; Fig 3b) from the ceiling topography (Fig 3a) to identify topographic anomalies (Fig 3c). A 98 percentile threshold (vertical red lines shown in Fig 4) was then applied to the histograms of these anomalies (Fig 4) to locate the stalactites (Fig 3d).
5. Stalactite positions were validated with field photographs.
6. Statistical properties of stalactites were calculated (Table 1).
7. We then plot stalactite length vs diameter, which signifies the most common geometrical properties of stalactites in a particular site (Fig 5, left). Lastly, stalactite lengths are plotted against ceiling elevation for all three sites in order to develop a relationship between stalactite length and the hydraulic gradient (Fig 5, right).

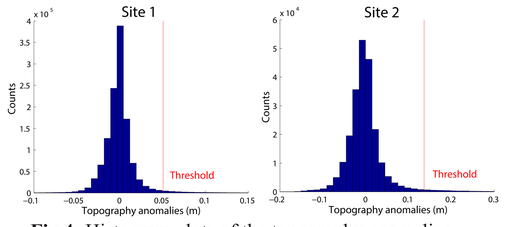

Fig 4: Histogram plots of the topography anomalies

Table 1: Stalactites properties from Lidar data analysis

Stalactites properties	Site 1	Site 2	Site 3
Ceiling dimension	19 m by 6.4 m	4.5 m by 5.0 m	8.0 m by 6.9 m
Threshold (m)	0.0508	0.1365	0.1397
Total number of stalactites	2010	372	465
Density of stalactites per m^2	17	17	8
Maximum diameter of one stalactite (cm)	34.4	26.6	51.9
Minimum diameter of one stalactite (cm)	1.1	1.1	1.1
Average length of stalactites (cm)	4.93	10.43	10.57
Maximum aspect ratio of stalactites	24.0	24.0	16.0
Minimum aspect ratio of stalactites	1.0	1.0	1.0
Average aspect ratio of stalactites	7.6	4.5	4.4

8. We differentiate various types of flow patterns using two stalactites properties i.e. aspect ratio and stalactite equivalent cross-sectional area (Fig 6).
9. Fig 7 shows linearity of stalactite clusters for both sites, as well as at an additional site 3, located 10m from site 2 near the opposite site of the same chamber. The analysis shows more linear clusters of stalactites are present in site 1 compared to other two sites, while site 2 mostly dominated by rounder groups of stalactites.

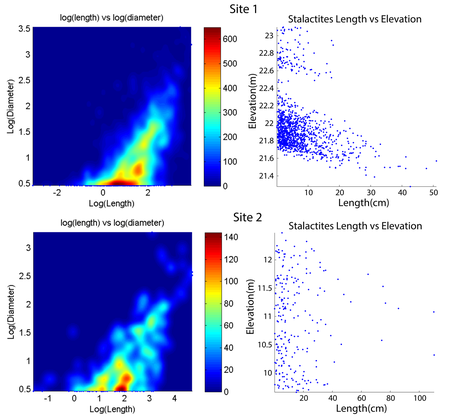

Fig 5: Stalactite length vs diameter plot with the application of kernel smoothing (Left). Colour scales represent density of points. Stalactite length vs ceiling elevation plots (Right). Longer stalactites tend to occur at comparatively lower ceiling elevations, which represent greater hydraulic gradients.

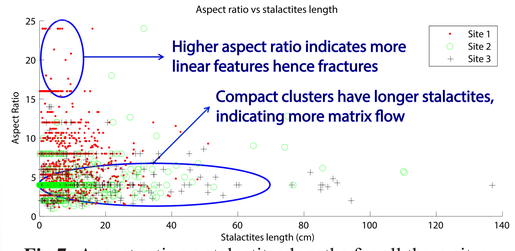

Fig 7: Aspect ratio vs stalactites lengths for all three sites

Work in progress

The physical and chemical properties of dripwater emerging from five of the stalactites have been monitored for the last 8 years as part of a cave monitoring program and more recently continuous drip rate measurements at 32 of these stalactites for past two years to further analyze other statistical tests and future exploration with stalagmate data.

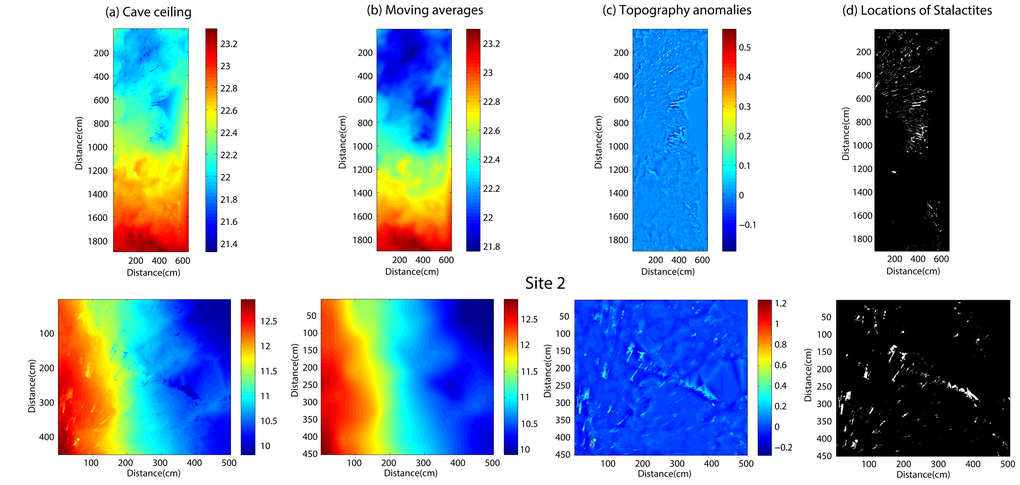

Fig 3: (a) Cave ceiling topography in 2D. (b) Moving averages with a window of 40x40 pixels grid. (c) Topographic anomaly maps. (d) Locations of stalactites. Isolate all pixels of topography anomalies with a deviation from the moving surfaces above a threshold. Colour scales represent elevations in meter of the ceiling points (Red specifies the higher elevation).

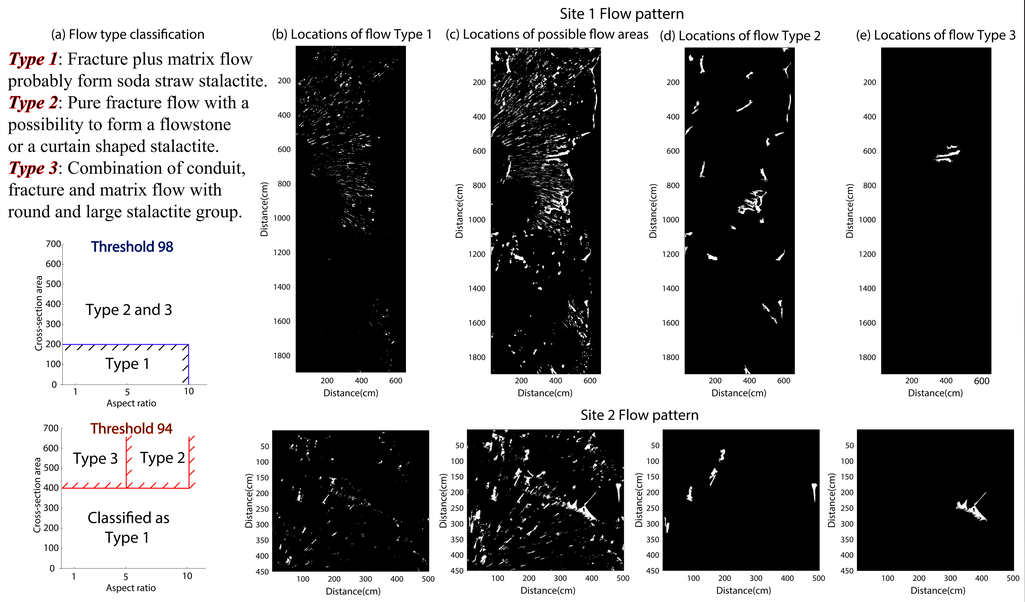

Fig 6: Flow patterns at different sites. (a) Definition of various flow type classification based on aspect ratio and cross-sectional area. Locations of flow Type 1 (shown in column b) are based on actual stalactite positions shown in Figure 3(d) using 98 percentile of the topography anomalies histogram (Figure 4). And we have used 94 percentile of the topography anomalies histogram to locate possible flow areas (c) to define flow Type 2 (d) and flow Type 3 (e).

Reference: Treble, P. C., C. Bradley, A. Wood, A. Baker, C. N. Jex, I. J. Fairchild, M. K. Gagan, J. Cowley, and C. Azcurra (2013), An isotopic and modelling study of flow paths and storage in Quaternary calcarenite, SW Australia: implications for speleothem paleoclimate records, Quaternary Science Reviews, 64, 90-103.